Signal Processing 129 (2016) 183–189

Contents lists available at ScienceDirect

Signal Processing

journal homepage: www.elsevier.com/locate/sigpro

# Improved DOA estimation based on real-valued array covariance using sparse Bayesian learning

Yi Wang [a,b], Minglei Yang [a,b,*], Baixiao Chen [a,b], Zhe Xiang [a,b]

[a] National Laboratory of Radar Signal Processing, Xidian University, Xi'an, Shaanxi 710071, China
[b] Collaborative Innovation Center of Information Sensing and Understanding at Xidian University, China

ARTICLE INFO

*Article history:*
Received 10 March 2016
Received in revised form
1 June 2016
Accepted 2 June 2016
Available online 4 June 2016

*Keywords:*
Direction of arrival
Unitary transformation
Sparse recovery
Sparse Bayesian learning

ABSTRACT

To further improve the efficiency of sparse Bayesian learning (SBL) for direction of arrival (DOA) estimation, a real-valued (unitary) formulation of covariance vector-based relevance vector machine (CV-RVM) technique is proposed in this paper. The covariance matrix of the sensor output is firstly transformed into a real-valued covariance matrix via unitary transformation, and the real-valued covariance matrix can be sparsely represented in a real-valued over-complete dictionary. Then the sparse Bayesian learning technique implemented in real domain is used to estimate the DOA. According to the property of the real-valued covariance matrix, unitary single measurement vector (USMV) CV-RVM for uncorrelated signals and unitary multiple measurement vector (UMMV) CV-RVM for correlated signals are developed, respectively. Due to the fact that the proposed methods are implemented in real domain and the snapshots are doubled via unitary transformation, the proposed methods have lower computational cost and better performance compared to the original SMV CV-RVM and MMV CV-RVM. Simulation results show the effectiveness of the proposed methods.



## 1. Introduction

Direction of arrival (DOA) estimation based on sensor arrays has been a hot topic in signal processing for decades, and it is widely applied to radar, sonar, and wireless communication [1]. Subspace based methods such as MUSIC [2] and ESPRIT [3] can estimate the DOA with high resolution. However, their performances decrease in low signal to noise ratio (SNR) and limited snapshot number scenarios.

In recent years, sparse reconstruction methods [4] play an important role in signal processing and have also been extended to DOA estimation scenario. By reconstructing the signals in an over-complete dictionary, the spatial sparsity of the signals can be exploited. Then the DOA estimation problem can be transformed to a special sparse recovery problem of single measurement vector (SMV) for single snapshot or multiple measurement vectors (MMV) for multiple snapshots. The sparse Bayesian learning (SBL) method [5] and the *p*-norm based methods [6–8] are two main categories of sparse reconstruction algorithms. The relevance vector machine (RVM)-DOA method is developed [9] with good performance and high resolution in low SNR and limited snapshot number scenarios.

To increase the degree of freedom (DOF) and improve angular resolution, a series of sparse reconstruction algorithms for DOA estimation based on the covariance matrix are developed [10–12]. The computational cost of SBL based methods mainly depends on the SNR, and the array covariance matrix has a higher SNR compared to the pure array output [13]. To improve the efficiency of RVM-DOA, SMV covariance vector-based relevance vector machine (CV-RVM) and MMV CV-RVM are proposed to implement the sparse recovery on the array covariance matrix [13]. In [14], off-grid block sparse Bayesian learning, which is used to estimate the off-grid DOAs, based on the array covariance matrix is presented. However, the methods proposed in [13,14] still suffer from high computational cost.

Real-valued formulations, which can be achieved by constructing invertible transformations that map centro-Hermitian matrices to real-valued matrices [15], have been used to reduce the computational complexity. For example, unitary ESPRIT [16] exploits the centro-Hermitian property of the forward–backward (FB) covariance matrix and has a better performance compared to ESPRIT with a reduced computational burden. The unitary formulations of the conventional subspace based DOA estimation methods, such as MUSIC, root-MUSIC, and MODE are also developed in various literatures [17,18].

In this paper, the unitary transformation is used to further improve the efficiency of SMV CV-RVM and MMV CV-RVM. The complex covariance matrix is firstly transformed to a real-valued

* Corresponding author at: National Laboratory of radar signal processing, Xidian University, China. Tel.: +86 13772029169, +86 29 88202248.
*E-mail address:* mlyang@xidian.edu.cn (M. Yang).

http://dx.doi.org/10.1016/j.sigpro.2016.06.002
0165-1684/

matrix. U(Unitary) SMV CV-RVM and UMMV CV-RVM are proposed for DOA estimation using sparse Bayesian leaning based on the real-valued covariance matrix. The computational costs of USMV CV-RVM and UMMV CV-RVM are reduced compared to the original SMV CV-RVM and UMMV CV-RVM. For uncorrelated signals, USMV CV−-RVM has a slightly better estimation accuracy than SMV CV-RVM. However, in correlated signals scenarios, the performance of UMMV CV-RVM is shown to be further improved.

*Notations*: The superscript $T$, and $H$ denote the transpose, and the conjugate transpose, respectively. The symbol $\otimes$ is used to denote the Kronecker product. $\mathrm{E}\{\cdot\}$ stands for the statistical expectation. $\boldsymbol{I}_M$ denotes the identity matrix with size $M$, and when the dimension is evident from the context, for simplicity, we just use $\boldsymbol{I}$. $|\boldsymbol{A}|$ represents the determinant of the matrix $\boldsymbol{A}$. $\mathrm{diag}(x)$ is a diagonal matrix with $x$ being its diagonal element, and $\mathrm{diag}(\boldsymbol{A})$ stands for a vector consisting of the diagonal elements of the marix $\boldsymbol{A}$. $\mathrm{vec}(\cdot)$ represents the vectorization operation which stacks the matrix column by column.

## 2. Signal model

Consider a uniform linear array (ULA) of $M$ sensors. Assume that $K$ narrowband signals from directions $\boldsymbol{\theta}=\left[\theta_1, \dots, \theta_k, \dots, \theta_K\right]$ impinge on the array. The sensor output can be represented by

$$\boldsymbol{x}(t)=\boldsymbol{A}\boldsymbol{s}(t)+\boldsymbol{n}(t), \qquad t=1, 2, \dots, N, \tag{1}$$

where $\boldsymbol{s}(t)=\left[s_1(t), s_2(t), \dots, s_K(t)\right]^T$ represents the signal vector, $\boldsymbol{A}=\left[\boldsymbol{a}(\theta_1), \boldsymbol{a}(\theta_2), \dots, \boldsymbol{a}(\theta_K)\right]$ denotes the array manifold, $\boldsymbol{a}(\theta_k)=\left[1, e^{j\frac{2\pi}{\lambda}d\ \sin\ \theta_k}, \dots, e^{j\frac{2\pi}{\lambda}md\ \sin\ \theta_k}, \dots, e^{j\frac{2\pi}{\lambda}d(M-1)\sin\ \theta_k}\right]^T$. $d$ is the inter-sensor spacing, $N$ is the snapshot number. $\lambda$ is the wavelength. The components of the noise vector $\boldsymbol{n}(t)$ are assumed independent and identically distributed (i.i.d.) additive white Gaussian noise with zero mean and variance $\sigma^2\boldsymbol{I}_M$, and are independent from the source signals.

The covariance matrix of the sensor outputs can be obtained by

$$\boldsymbol{R}=E\left\{\boldsymbol{x}(t)\boldsymbol{x}^H(t)\right\}=\boldsymbol{A}\boldsymbol{S}\boldsymbol{A}^H+\sigma^2\boldsymbol{I}_M, \tag{2}$$

where $\boldsymbol{S}$ denotes covariance matrix of the signals.

The covariance matrix can be calculated by its maximum likelihood estimation in practice

$$\hat{\boldsymbol{R}}=\frac{1}{N}\sum_{t=1}^{N}\boldsymbol{x}(t)\boldsymbol{x}^H(t). \tag{3}$$

When the signals are independent, $S=\mathrm{diag}\left\{\sigma_1^2, \sigma_2^2, \dots, \sigma_k^2, \dots, \sigma_K^2\right\}$, where $\sigma_k^2$ represents the source power of the $k$th signal. Vectorizing the covariance matrix (2), we obtain a covariance vector

$$\boldsymbol{y}=\mathrm{vec}(\boldsymbol{R})=\boldsymbol{A}^*\ \odot\ \boldsymbol{A}\boldsymbol{p}+\sigma^2\tilde{\boldsymbol{e}}, \tag{4}$$

where $\odot$ represents the Khatri–Rao product [19]. $p=\left[\sigma_1^2, \sigma_2^2, \dots, \sigma_k^2, \dots, \sigma_K^2\right]^T$, and $\tilde{\boldsymbol{e}}=\mathrm{vec}(\boldsymbol{I}_M)$. Note that $\boldsymbol{p}$ is a real and nonnegative vector.

Discretize the angle domain using a grid sampling $\boldsymbol{\Theta}=\left[\tilde{\theta}_1, \tilde{\theta}_2, \dots, \tilde{\theta}_D\right]$, where $D$ is the grid number, $D\gg M$, and $\boldsymbol{\Theta}$ contains the directions of interest. The covariance vector can be represented by

$$y=B(\boldsymbol{\Theta})\tilde{\boldsymbol{p}}+\sigma^2\tilde{\boldsymbol{e}}, \tag{5}$$

where

$$\boldsymbol{B}(\boldsymbol{\Theta})=\tilde{\boldsymbol{A}}^*(\boldsymbol{\Theta})\ \odot\ \tilde{\boldsymbol{A}}(\boldsymbol{\Theta})=\left[\boldsymbol{a}^*(\tilde{\theta}_1)\otimes\boldsymbol{a}(\tilde{\theta}_1), \dots, \boldsymbol{a}^*(\tilde{\theta}_D)\otimes\boldsymbol{a}(\tilde{\theta}_D)\right], \tag{6}$$

$$\tilde{A}(\boldsymbol{\Theta})=\left[\boldsymbol{a}(\tilde{\theta}_1), \boldsymbol{a}(\tilde{\theta}_2), \dots, \boldsymbol{a}(\tilde{\theta}_D)\right]. \tag{7}$$

$\boldsymbol{B}(\boldsymbol{\Theta})$ can be interpreted as an over complete dictionary of directions of interest, and $\tilde{\boldsymbol{p}}$ is a $K$ sparse vector, where the nonzero entries of $\tilde{\boldsymbol{p}}$ are corresponding to the true DOAs. It is a zero-padded extension of $\boldsymbol{p}$ from $\boldsymbol{\theta}$ to $\boldsymbol{\Theta}$.

## 3. Covariance vector based unitary SBL

To improve the efficiency of SMV CV-RVM, the unitary formulation of SMV CV-RVM is developed in this section. The covariance matrix should be transformed to a real-valued matrix firstly.

### 3.1. The transformation of the real-valued covariance matrix

By using the centro-Hermitian property of the ULA, the complex covariance matrix of the received data of the ULA can be transformed into a real-valued matrix of the same size [18]. First, we define an $\boldsymbol{Q}$ as

$$Q=\frac{1}{\sqrt{2}}\begin{bmatrix}\boldsymbol{I} & j\boldsymbol{I}\\ \boldsymbol{J} & -j\boldsymbol{J}\end{bmatrix}\cdot(M\cdot\text{is even})\cdot\text{or}\cdot Q=\frac{1}{\sqrt{2}}\begin{bmatrix}\boldsymbol{I} & \boldsymbol{0} & j\boldsymbol{I}\\ \boldsymbol{0}^T & \sqrt{2} & \boldsymbol{0}^T\\ \boldsymbol{J} & \boldsymbol{0} & -j\boldsymbol{J}\end{bmatrix}(M\cdot\text{is odd}) \tag{8}$$

Following [18], we introduce the data matrix

$$T(\boldsymbol{X})=\boldsymbol{Q}_M^H\left[\boldsymbol{x}\quad \boldsymbol{J}_M\boldsymbol{x}^*\boldsymbol{J}_N\right]\boldsymbol{Q}_{2N}, \tag{9}$$

where $\boldsymbol{J}_M$ is an $M\times M$ exchange matrix with ones on its anti-diagonal and zeros elsewhere. To 'double' the number of snapshots, the centro-Hermitian property is forced by FB averaging [16,18]

$$\hat{\boldsymbol{R}}_{FB}=\frac{1}{2}\left(\hat{\boldsymbol{R}}+\boldsymbol{J}\hat{\boldsymbol{R}}^*\boldsymbol{J}\right)=A\tilde{\boldsymbol{S}}\boldsymbol{A}^H+\sigma^2\boldsymbol{I}_M, \tag{10}$$

where $\tilde{\boldsymbol{S}}=\frac{1}{2}\left(\boldsymbol{S}+\Delta\boldsymbol{S}^*\Delta^H\right)$, and $\boldsymbol{\Delta}=\mathrm{diag}\left\{e^{-j\frac{2\pi}{\lambda}d(M-1)\sin\ \theta_1}, e^{-j\frac{2\pi}{\lambda}d(M-1)\sin\ \theta_2}, \dots, e^{-j\frac{2\pi}{\lambda}d(M-1)\sin\ \theta_K}\right\}$.

Then we can obtain the real-valued matrix as follows

$$\boldsymbol{R}_r=\frac{1}{2N}T(\boldsymbol{X})T^H(\boldsymbol{X})=\frac{1}{2}\boldsymbol{Q}^H\left(\hat{\boldsymbol{R}}+\boldsymbol{J}_M\hat{\boldsymbol{R}}^*\boldsymbol{J}_M\right)Q=\mathrm{Re}\left\{\boldsymbol{Q}^H\hat{\boldsymbol{R}}Q\right\}. \tag{11}$$

Vectorizing the real-valued matrix, we obtain that $\boldsymbol{y}_r=\mathrm{vec}(\boldsymbol{R}_r)$. Due to the influence of finite snapshots, there is a perturbation of the estimated covariance vector [13]. The perturbation (estimation error) of the covariance vector $\boldsymbol{y}$ and the real-valued covariance vector $\boldsymbol{y}_r$ are defined as $\boldsymbol{\xi}=\boldsymbol{y}-\hat{\boldsymbol{y}}$ and $\boldsymbol{\xi}_r=\boldsymbol{y}_r-\hat{\boldsymbol{y}}_r$, respectively. The perturbation can be treated as the colored noise of the covariance vector. To use the SBL technique, the covariance matrix of the perturbation should be analyzed.

### 3.2. The perturbation of the covariance vector

Here we first consider the case when $\boldsymbol{M}$ is even, and the case when $\boldsymbol{M}$ is odd can be obtained in a similar way. $\boldsymbol{R}$ can be partitioned as follows

$$R=\begin{bmatrix}\boldsymbol{R}_{11} & \boldsymbol{R}_{12}\\ \boldsymbol{R}_{21} & \boldsymbol{R}_{22}\end{bmatrix}, \tag{12}$$

Then,

$$\boldsymbol{Q}^H\mathrm{RQ}=\frac{1}{2}\begin{bmatrix}\boldsymbol{R}_{11}+\boldsymbol{R}_{12}\boldsymbol{J}+\boldsymbol{J}\boldsymbol{R}_{21}+\boldsymbol{J}\boldsymbol{R}_{22}\boldsymbol{J} & j\boldsymbol{R}_{11}-j\boldsymbol{R}_{12}\boldsymbol{J}+j\boldsymbol{J}\boldsymbol{R}_{21}-j\boldsymbol{J}\boldsymbol{R}_{22}\boldsymbol{J}\\ -j\boldsymbol{R}_{11}-j\boldsymbol{R}_{12}\boldsymbol{J}+j\boldsymbol{J}\boldsymbol{R}_{21}+j\boldsymbol{J}\boldsymbol{R}_{22}\boldsymbol{J} & \boldsymbol{R}_{11}-\boldsymbol{R}_{12}\boldsymbol{J}-\boldsymbol{J}\boldsymbol{R}_{21}+\boldsymbol{J}\boldsymbol{R}_{22}\boldsymbol{J}\end{bmatrix}. \tag{13}$$

From (13) we observe that each partition of $\boldsymbol{Q}^H\boldsymbol{R}\boldsymbol{Q}$ is a linear

combination of the four partitions of $\boldsymbol{R}$. Therefore, $\mathrm{vec}(\boldsymbol{Q}^H\boldsymbol{R}\boldsymbol{Q})$ is also a linear combination of $\mathrm{vec}(\boldsymbol{R})$, and their relationship can be represented as

$$\mathrm{vec}(\boldsymbol{Q}^H\boldsymbol{R}\boldsymbol{Q}) = \boldsymbol{P}\mathrm{vec}(\boldsymbol{R}), \tag{14}$$

where $P = T \otimes \boldsymbol{Q}^H$, and $T = \frac{1}{\sqrt{2}}\begin{bmatrix} \boldsymbol{I} & \boldsymbol{J} \\ j\boldsymbol{I} & -j\boldsymbol{J} \end{bmatrix}$. Actually, we can obtain $\boldsymbol{P}$ off-line according to the number of sensors.

From Eqs. (11) and (14), we obtain that

$$\boldsymbol{\xi}_r = \frac{1}{2}\left(P\boldsymbol{\xi} + (P\boldsymbol{\xi})^*\right), \tag{15}$$

According to [13], $\boldsymbol{\xi}$ follows a complex Gaussian distribution $\boldsymbol{\xi} \backsim C\mathcal{N}(\boldsymbol{0}, \boldsymbol{W})$, where $\boldsymbol{W} = \frac{1}{N}\boldsymbol{R}^T \otimes \boldsymbol{R}$.

Using Gaussian distribution properties of $\boldsymbol{\xi}$, the covariance matrix of the perturbation of the real-valued matrix can be obtained

$$\begin{aligned} \mathrm{E}\left\{\boldsymbol{\xi}_r\boldsymbol{\xi}_r^T\right\} &= \frac{1}{4}\mathrm{E}\left\{\left(P\boldsymbol{\xi} + (P\boldsymbol{\xi})^*\right)\left(P\boldsymbol{\xi} + (P\boldsymbol{\xi})^*\right)^H\right\} \\ &= \frac{1}{4}\mathrm{E}\left\{P\boldsymbol{\xi}\boldsymbol{\xi}^HP^H + P\boldsymbol{\xi}\boldsymbol{\xi}^TP^T + \boldsymbol{P}^*\boldsymbol{\xi}^*\boldsymbol{\xi}^HP^H + \boldsymbol{P}^*\boldsymbol{\xi}^*\boldsymbol{\xi}^TP^T\right\} \\ &= \frac{1}{4}\left(\boldsymbol{P}\boldsymbol{W}\boldsymbol{P}^H + \boldsymbol{P}^*\boldsymbol{W}^T\boldsymbol{P}^T\right) = \frac{1}{2}\mathrm{Re}\left\{\boldsymbol{P}\boldsymbol{W}\boldsymbol{P}^H\right\} = \boldsymbol{C}, \end{aligned} \tag{16}$$

where $\boldsymbol{C}$ denotes the real-valued covariance matrix of the perturbation $\boldsymbol{\xi}_r$, and we obtain that $\boldsymbol{\xi}_r \sim \mathcal{N}(0, C)$. As the covariance matrix of the perturbation is known, we can develop the SBL technique using the real-valued matrix.

### 3.3. The SBL technique for DOA estimation using the real-valued matrix

Similar as (6), the real-valued over-complete directional dictionary can be represented by

$$\boldsymbol{b}(\tilde{\theta}) = \boldsymbol{P}\left(\boldsymbol{a}^*(\tilde{\theta}) \otimes \boldsymbol{a}(\tilde{\theta})\right), \tag{17}$$

$$\boldsymbol{B}_r = \boldsymbol{B}_r(\boldsymbol{\Theta}) = \boldsymbol{P}(\tilde{\boldsymbol{A}}^* \odot \tilde{\boldsymbol{A}}) = \left[\boldsymbol{b}(\tilde{\theta}_1), \boldsymbol{b}(\tilde{\theta}_2), \ldots, \boldsymbol{b}(\tilde{\theta}_D)\right]. \tag{18}$$

Thus the real-valued covariance matrix vector can be sparsely represented by

$$\hat{\boldsymbol{y}}_r = \boldsymbol{B}_r\tilde{\boldsymbol{p}} + \sigma^2\tilde{\boldsymbol{e}} + \boldsymbol{\xi}_r. \tag{19}$$

To reduce the effect of the noise and make the relationship between the vector and the signal directions clearer, we remove the noise component from $\hat{\boldsymbol{y}}_r$ firstly. The noise variance $\hat{\sigma}^2$ can be estimated by the mean of the minimum $M - K$ eigenvalues of $\hat{\boldsymbol{R}}_r$, that is

$$\hat{\sigma}^2 = \frac{1}{M-K}\sum_{m=K+1}^{M}\lambda_m, \tag{20}$$

where $\lambda_m$ denotes the $m$th eigenvalues of $\hat{\boldsymbol{R}}_r$, and $\lambda_m$ is sorted in descending order.

After removing the noise component, we obtain that

$$\bar{\boldsymbol{y}}_r = \mathrm{vec}\left(\bar{\boldsymbol{R}}_r\right) = \mathrm{vec}\left(\hat{\boldsymbol{R}}_r - \hat{\sigma}^2\boldsymbol{I}_M\right) = \hat{\boldsymbol{y}}_r - \hat{\sigma}^2\tilde{\boldsymbol{e}}, \tag{21}$$

Although $\tilde{\boldsymbol{p}}$ is not smaller than zero, this prior information hinders the implementation of the SBL technique. Following the similar procedure of SBL [5,13], we assume that $\tilde{\boldsymbol{p}} \backsim \mathcal{N}(0, \boldsymbol{\Gamma})$, where $\mathcal{N}(0, \boldsymbol{\Gamma})$ denotes the Gaussian distribution with mean $\boldsymbol{0}$ and covariance matrix $\boldsymbol{\Gamma}$, and $\boldsymbol{\Gamma} = \mathrm{diag}\{\boldsymbol{\gamma}\}$, $\boldsymbol{\gamma} = \{\gamma_1, \gamma_2, \ldots, \gamma_D\}$. $\boldsymbol{\gamma}$ is a hyper parameter that controls the nonzero rows of $\tilde{\boldsymbol{p}}$. When $\gamma_i$ is zero, the corresponding row of $\tilde{\boldsymbol{p}}$ becomes zero. Once we obtain $\boldsymbol{\gamma}$, we can form a spatial spectrum of the proposed method using $\boldsymbol{\gamma}$. The number of sources is assumed known in this paper, which can be obtained using the AIC criteria [20]. Then the DOAs of the signals can be obtained from the locations of the $K$ highest peaks.

In [5], an evidence procedure is exploited to perform the Bayesian inference since the exact posterior distribution cannot be explicitly calculated. To estimate these hyper parameters, evidence maximization (EM) method is employed in SBL technique [5].

The cost function is defined as follows [9,13]

$$L(\Theta) = \bar{\boldsymbol{y}}_r^T\boldsymbol{\Sigma}_{y_r}^{-1}\bar{\boldsymbol{y}}_r + \ln\left|\boldsymbol{\Sigma}_{y_r}\right|, \tag{22}$$

where $\boldsymbol{\Sigma}_{y_r} = C + \boldsymbol{B}_r\boldsymbol{\Gamma}\boldsymbol{B}_r$.

Treating the vector $\tilde{\boldsymbol{p}}$ as hidden variables, the expectation of posterior probability is maximized iteratively when given $\tilde{\boldsymbol{p}}$ and hyper parameters $\boldsymbol{\gamma}$. We employ the expectation–maximization (EM) method to maximize $p\left(\bar{\boldsymbol{y}}_r, \tilde{\boldsymbol{p}}; \boldsymbol{\gamma}^{q+1}\right)$, which is equivalent to minimizing $-\ln\left(p\left(\bar{\boldsymbol{y}}_r, \tilde{\boldsymbol{p}}; \boldsymbol{\gamma}^{q+1}\right)\right)$. According to the Bayesian formula, the cost function can be simplified as

$$\begin{aligned} \tilde{L} &= \mathrm{E}_{\tilde{\boldsymbol{p}}|\bar{\boldsymbol{y}}_r}\left(\ln\ p\left(\bar{\boldsymbol{y}}_r, \tilde{\boldsymbol{p}}; \boldsymbol{\gamma}^{q+1}\right)\right) \\ &= \mathrm{E}_{\tilde{\boldsymbol{p}}|\bar{\boldsymbol{y}}_r}\left(\ln\ p\left(\bar{\boldsymbol{y}}_r|\tilde{\boldsymbol{p}}; \boldsymbol{C}\right)\right) + \mathrm{E}_{\tilde{\boldsymbol{p}}|\bar{\boldsymbol{y}}_r}\left(\ln\ p\left(\tilde{\boldsymbol{p}}; \boldsymbol{\gamma}^{q+1}\right)\right), \end{aligned} \tag{23}$$

where the subscript '$a|b$' denotes the condition of $a$ given $b$. The posterior distribution of $\tilde{\boldsymbol{p}}$ follows a Gaussian distribution [5,9]

$$\tilde{\boldsymbol{p}} \sim \mathcal{N}\left(\boldsymbol{u}_{\tilde{\boldsymbol{p}}}, \boldsymbol{\Sigma}_{\tilde{\boldsymbol{p}}}\right), \tag{24}$$

where the mean and covariance matrix are respectively

$$\boldsymbol{u}_{\tilde{\boldsymbol{p}}} = \boldsymbol{\Gamma}\boldsymbol{B}_r\left[\boldsymbol{C} + \boldsymbol{B}_r\boldsymbol{\Gamma}\boldsymbol{B}_r^T\right]^{-1}\bar{\boldsymbol{y}}_r, \tag{25}$$

$$\boldsymbol{\Sigma}_{\tilde{\boldsymbol{p}}} = \boldsymbol{\Gamma} - \boldsymbol{\Gamma}\boldsymbol{B}_r^T\left[\boldsymbol{C} + \boldsymbol{B}_r\boldsymbol{\Gamma}\boldsymbol{B}_r^T\right]^{-1}\boldsymbol{B}_r\boldsymbol{\Gamma}. \tag{26}$$

The first item of (23) has no connection with $\boldsymbol{\gamma}$, thus the cost function of $\boldsymbol{\gamma}$ can be simplified as

$$L(\boldsymbol{\gamma}) = \mathrm{E}_{\tilde{\boldsymbol{p}}|\bar{\boldsymbol{y}}_r}\left(\ln\ p\left(\tilde{\boldsymbol{p}}; \boldsymbol{\gamma}^{q+1}\right)\right) = \ln|\boldsymbol{\Gamma}| + \mathrm{Tr}\left(\tilde{\boldsymbol{p}}^T\boldsymbol{\Gamma}^{-1}\tilde{\boldsymbol{p}}\right). \tag{27}$$

Let the derivative of (27) with respect to $\gamma_i$ be zero, i.e., $\partial L(\boldsymbol{\gamma})/\partial\gamma_i = 0$. We can obtain the update rule of the hyper parameter

$$\gamma_i = |\boldsymbol{u}_i|^2 + \left(\boldsymbol{\Sigma}_{\tilde{\boldsymbol{p}}}\right)_{i,i}, \tag{28}$$

where $\boldsymbol{u}_i$ is the $i$th row of $\boldsymbol{u}_{\tilde{\boldsymbol{p}}}$, and $\left(\boldsymbol{\Sigma}_{\tilde{\boldsymbol{p}}}\right)_{i,i}$ is the $i$th diagonal element of $\boldsymbol{\Sigma}_{\tilde{\boldsymbol{p}}}$.

### 3.4. Refined procedure

To reduce the computational complexity and the quantization error, we adopt the following refined procedure to improve the DOA estimation performance [9,13].

Let $(\boldsymbol{\Theta})_{-k} = \boldsymbol{\Theta}/\theta_k$, which means removing $\theta_k$ from $\boldsymbol{\Theta}$. Similarly, $\boldsymbol{\gamma}_{-k} = \boldsymbol{\gamma}/\gamma_k$, $\boldsymbol{\Gamma}_{-k} = \mathrm{diag}\{\boldsymbol{\gamma}_{-k}\}$, $\boldsymbol{\Sigma}_{-k} = (\boldsymbol{B}_r)_{-k}\boldsymbol{\Gamma}_{-k}(\boldsymbol{B}_r)_{-k}^T + \boldsymbol{C}$. $\boldsymbol{\Sigma}_{-k}$ can be deemed as the covariance matrix of the estimation error of the other $K-1$ signal components in $\boldsymbol{y}_r$ except the $k$th one.

By substituting $\boldsymbol{\Sigma}_{-k}$ into (22), we can obtain the following objective function

$$L(\beta_k, \theta) = \ln\left|\Sigma_{-k} + \beta_k\boldsymbol{b}(\theta)\boldsymbol{b}^T(\theta)\right| + \bar{\boldsymbol{y}}_r^T\left[\Sigma_{-k} + \beta_k\boldsymbol{b}(\theta)\boldsymbol{b}^T(\theta)\right]^{-1}\bar{\boldsymbol{y}}_r. \tag{29}$$

The estimation of $\beta_k$ can be derived according to $\partial L(\beta_k, \theta)/\partial\beta_k = 0$

$$\beta_k = \frac{\boldsymbol{b}^T(\theta)\Sigma_{-k}^{-1}\left[\bar{\boldsymbol{y}}_r\bar{\boldsymbol{y}}_r^T - \Sigma_{-k}\right]\Sigma_{-k}^{-1}\boldsymbol{b}(\theta)}{\left(\boldsymbol{b}^T(\theta)\Sigma_{-k}^{-1}\boldsymbol{b}(\theta)\right)^2}. \tag{30}$$

Then substituting (30) into $\partial L(\beta_k, \theta)/\partial\theta = 0$ yields

$$g(\theta) = \boldsymbol{b}(\theta)^T \Sigma_{-k}^{-1}\Big[\boldsymbol{b}(\theta)\boldsymbol{b}(\theta)^T \Sigma_{-k}^{-1}\bar{\boldsymbol{y}}_r\bar{\boldsymbol{y}}_r^T - \bar{\boldsymbol{y}}_r\bar{\boldsymbol{y}}_r^T \Sigma_{-k}^{-1}\boldsymbol{b}(\theta)\boldsymbol{b}(\theta)^T\Big]\Sigma_{-k}^{-1}\frac{d\big[\boldsymbol{b}(\theta)\big]}{d\theta} = 0. \tag{31}$$

The final refined DOA can be obtained by the following 1-D searching

$$\theta = \min_{\theta\in\Omega_k}|g(\theta)|, \tag{32}$$

where $\Omega_k$ represents the peak scope of the $k$th signal, and the DOA can also be obtained from the peak of the spectrum forms from $1/g(\theta)$.

In summary, Eqs. (25), (26) (28) and (31) are implemented in real-valued domain and thus is named unitary single measurement vector covariance vector-based relevance vector machine (USMV CV-RVM).

## 4. The SBL technique for correlated signals

For correlated signals, the covariance vector (4) cannot be sparsely represented by a single array manifold and the DOA cannot be estimated with the same way as the uncorrelated signals. Each column of the covariance matrix $\boldsymbol{R}_r$ share the identical base $\boldsymbol{Q}^H\boldsymbol{A}$, therefore we can recover the sparse vector of every column of the real-valued matrix jointly.

In the case of correlated signals, the real-valued covariance matrix can be represented as

$$\boldsymbol{R}_r = \boldsymbol{Q}^H A\tilde{\boldsymbol{S}}\boldsymbol{A}^H\boldsymbol{Q} + \sigma^2\boldsymbol{I}_M = \boldsymbol{Q}^H A\Lambda H + \sigma^2\boldsymbol{I}_M, \tag{33}$$

where $H = \big[\boldsymbol{h}_1, \boldsymbol{h}_2, \dots, \boldsymbol{h}_m, \dots, \boldsymbol{h}_M\big]$ is a $M\times M$ real-valued matrix, $\Lambda = \mathrm{diag}\Big\{e^{-j\frac{\pi}{\lambda}(M-1)d\ \sin\ \theta_1}, e^{-j\frac{\pi}{\lambda}(M-1)d\ \sin\ \theta_2}, \dots, e^{-j\frac{\pi}{\lambda}(M-1)d\ \sin\ \theta_K}\Big\}$.

$\bar{\boldsymbol{y}}_r$ can be partitioned into $M$ vectors with the same length

$$\bar{\boldsymbol{y}}_r = \Big[\bar{\boldsymbol{y}}_{r1}^T, \bar{\boldsymbol{y}}_{r2}^T, \dots, \bar{\boldsymbol{y}}_{rm}^T, \dots, \bar{\boldsymbol{y}}_{rM}^T\Big]^T, \tag{34}$$

where $\bar{\boldsymbol{y}}_{rm} = \bar{\boldsymbol{R}}_{rm}$, i.e., the $m$th column of $\bar{\boldsymbol{R}}_r$. The perturbation $\boldsymbol{\xi}_r$ can be partitioned as $\boldsymbol{\xi}_r = \big[\boldsymbol{\xi}_{r1}^T, \boldsymbol{\xi}_{r2}^T, \dots, \boldsymbol{\xi}_{rm}^T, \dots, \boldsymbol{\xi}_{rM}^T\big]^T$. Then we can obtain that

$$\mathrm{E}\Big\{\boldsymbol{\xi}_{rm}\boldsymbol{\xi}_{rm}^T\Big\} = c_{rm}\boldsymbol{R}_r, \tag{35}$$

where $c_{rm}$ is a real constant, and it is the $m$th diagonal element of the matrix $\frac{1}{2N}\boldsymbol{T}\boldsymbol{R}^T\boldsymbol{T}^H$. The detailed derivation is provided in the Appendix A.

The $m$th $M\times 1$ subvector of $\bar{\boldsymbol{y}}_r$ can be sparsely represented by

$$\bar{\boldsymbol{y}}_{rm} = \boldsymbol{A}'(\boldsymbol{\Theta})\tilde{\boldsymbol{h}}_m + \boldsymbol{\xi}_{rm}, \tag{36}$$

where $\boldsymbol{A}'(\boldsymbol{\Theta}) = \boldsymbol{Q}^H\tilde{\boldsymbol{A}}(\boldsymbol{\Theta})\tilde{\Lambda}$ , and $\tilde{\boldsymbol{h}}_m$ is a zero-padded extension of $\boldsymbol{h}_m$ from $\boldsymbol{\theta}$ to $\boldsymbol{\Theta}$. From (35), we can obtain that $\boldsymbol{\xi}_{rm}\sim\mathcal{N}(0, c_{rm}\boldsymbol{R}_r)$.

Once we obtain $c_{rm}$ at every column. Define $G = diag\Big\{\sqrt{c_{r1}}, \sqrt{c_{r2}}, \dots, \sqrt{c_{rm}}, \dots, \sqrt{c_{rM}}\Big\}$, then

$$\tilde{\boldsymbol{R}}_r = \bar{\boldsymbol{R}}_r\boldsymbol{G}^{-1}, \tag{37}$$

Assume that $\tilde{\boldsymbol{h}}_m/\sqrt{c_{rm}}\sim\mathcal{N}(0, \boldsymbol{\Gamma})$. The sparse recovery problem of (36) can be seen as a MMV problem as in [13,21]. The following SBL procedure can be used to solve the problem efficiently

$$\boldsymbol{U} = \boldsymbol{\Gamma}\boldsymbol{A}'(\boldsymbol{\Theta})\Big[\boldsymbol{R}_r + \boldsymbol{A}'(\boldsymbol{\Theta})\boldsymbol{\Gamma}\boldsymbol{A}'(\boldsymbol{\Theta})^T\Big]^{-1}\tilde{\boldsymbol{R}}_r, \tag{38}$$

$$\boldsymbol{\Sigma} = \boldsymbol{\Gamma} - \boldsymbol{\Gamma}\boldsymbol{A}'(\boldsymbol{\Theta})^T\Big[\boldsymbol{R}_r + \boldsymbol{A}'(\boldsymbol{\Theta})\boldsymbol{\Gamma}\boldsymbol{A}'(\boldsymbol{\Theta})^T\Big]^{-1}\boldsymbol{A}'(\boldsymbol{\Theta})\boldsymbol{\Gamma}, \tag{39}$$

$$\gamma_i = \boldsymbol{U}_i\boldsymbol{U}_i^T/M + (\boldsymbol{\Sigma})_{i,i}. \tag{40}$$

Using the same way as the uncorrelated signals, when the SBL method terminates, the following 1-D searching procedure can be used to refine the results, and

$$g(\theta) = \boldsymbol{a}'(\theta)\boldsymbol{\Sigma}_{-k}^{-1}\Big[\boldsymbol{a}'(\theta)\boldsymbol{a}'^T(\theta)\boldsymbol{\Sigma}_{-k}^{-1}\tilde{\boldsymbol{R}}_r\tilde{\boldsymbol{R}}_r^T - \tilde{\boldsymbol{R}}_r\tilde{\boldsymbol{R}}_r^T\boldsymbol{\Sigma}_{-k}^{-1}\boldsymbol{a}'(\theta)\boldsymbol{a}'^T(\theta)\Big]\boldsymbol{\Sigma}_{-k}^{-1}\frac{d\big[\boldsymbol{a}'(\theta)\big]}{d\theta}, \tag{41}$$

where $\boldsymbol{a}'(\theta) = \boldsymbol{Q}^H\boldsymbol{a}(\theta)e^{-j\frac{\pi}{\lambda}(M-1)d\ \sin\ \theta}$.

Eqs. (38–41) are the SBL technique of real-valued covariance matrix for correlated signals, and thus is named unitary multiple measurement vector covariance vector-based relevance vector machine (UMMV CV-RVM).

Because of $\boldsymbol{P}$ and $\boldsymbol{Q}$ are nonsingular matrix, we can obtain that $\mathrm{Spark}(\boldsymbol{B}_r) = \mathrm{Spark}(\boldsymbol{B}(\boldsymbol{\Theta}))$ and $\mathrm{Spark}\big(\boldsymbol{A}'(\boldsymbol{\Theta})\big) = \mathrm{Spark}\big(\tilde{\boldsymbol{A}}(\boldsymbol{\Theta})\big)$, where $\mathrm{Spark}(\cdot)$ denotes the smallest integer of columns of the matrix that are linearly dependent. For ULA, the degree of freedom of $y_r$ is $2M-1$ when the signals are uncorrelated, i.e., the dimension of $y_r$ is $2M-1$ after removing the duplication elements. According to [13], for uncorrelated narrowband signals, USMV CV-RVM can estimate $M-1$ sources. From [22], we know that the number of nonzero rows which can be sparsely recovered in MMV sparse recovery problems is smaller than $\big(\mathrm{Spark}(\boldsymbol{A}'(\boldsymbol{\Theta}))-1+\mathrm{rank}(\boldsymbol{H})\big)/2$. From the previous assumption, we can obtain $\mathrm{Spark}(\boldsymbol{A}'(\boldsymbol{\Theta})) = M+1$ for narrowband DOA estimation problem according to the Vandermonde structure of the dictionary matrix. For complete coherent sources, UMMV CV-RVM can estimate $\frac{M}{2}$ sources.

## 5. Simulation results

Computer simulations are conducted in this section to verify the effectiveness of the proposed methods and the proposed methods are compared with MUSIC [2], SSMUSIC [23], SMV CV-RVM and MMV CV-RVM [13]. A ULA of 6 sensors is used in all simulations and the inter-element spacing of the ULA is a half wavelength. The spatial space is divided into 181 grids from $-90^\circ$ to $90^\circ$ with $1^\circ$ interval to obtain the direction set $\boldsymbol{\Theta}$. The SBL based methods will not terminate until the iterations reach 3000 or $\|\gamma^{q+1}-\gamma^q\|_2/\|\gamma^q\|_2 \le 10^{-4}$. The precision of the refined procedure, MUSIC, and SSMUSIC is $10^{(-\mathrm{SNR}/20-1)}$ degree.

First we assume that two uncorrelated narrowband signals from directions $-5.3^\circ$ and $4.9^\circ$ imping on the ULA. The spatial spectrums of MUSIC, SMV CV-RVM, USMV CV-RVM are shown in Fig. 1, where the SNR is 0 dB and the snapshot number is 100. Fig. 1 (a) shows that the MUSIC algorithm cannot resolve the two sources, but the SBL based methods can estimate the DOAs at the grid $-5^\circ$ and $5^\circ$. The refined DOA estimation in Fig. 1(b) shows the DOAs at $-5.3^\circ$ and $4.9^\circ$, which demonstrates that the refined procedure can further improve the DOA estimation accuracy.

In the second simulation, two uncorrelated narrowband signals from directions $-5^\circ+v$ and $5^\circ+v$ imping on the ULA, where $v$ is a random value which is uniformly distributed within $\big[-0.5^\circ, 0.5^\circ\big]$. We use root mean square error (RMSE) to evaluate the performance of the algorithms. RMSE is defined as

$$\mathrm{RMSE} = \sqrt{\frac{1}{WK}\sum_{w=1}^{W}\sum_{k=1}^{K}\Big(\hat{\theta}_k^{(w)} - \theta_k^{(w)}\Big)^2}, \tag{42}$$

where $\hat{\theta}_k^{(w)}$ and $\theta_k^{(w)}$ are the estimated and true DOA of the $k$th signal at the $w$th trial, and $W$ is the number of Monte Carlo trials. All the following results about RMSE are obtained by 300 Monte Carlo trials. Figs. 2 and 3 show the RMSEs of MUSIC, SMV CV-RVM,

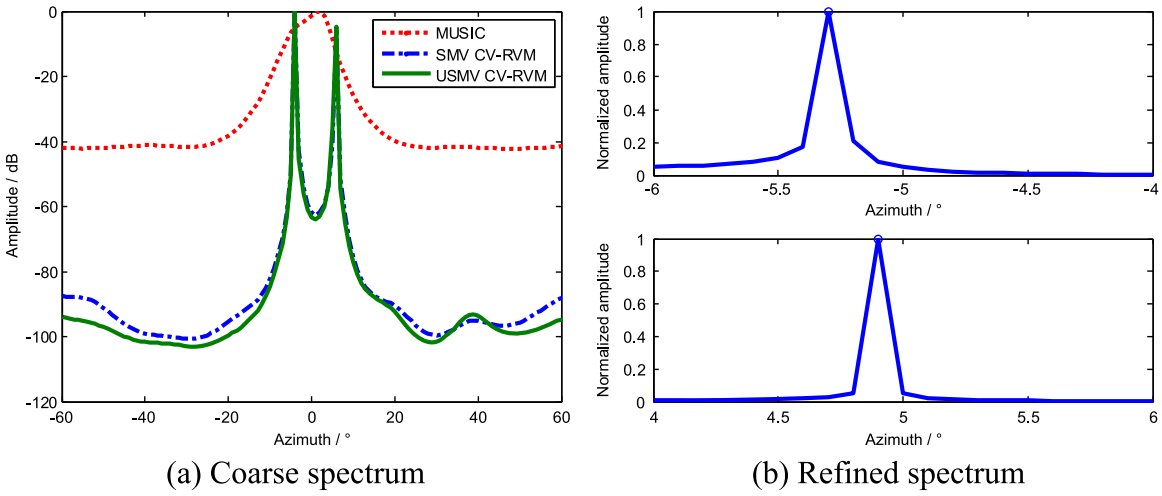


(a) Coarse spectrum (b) Refined spectrum

**Fig. 1.** Spatial spectrum of the various methods.

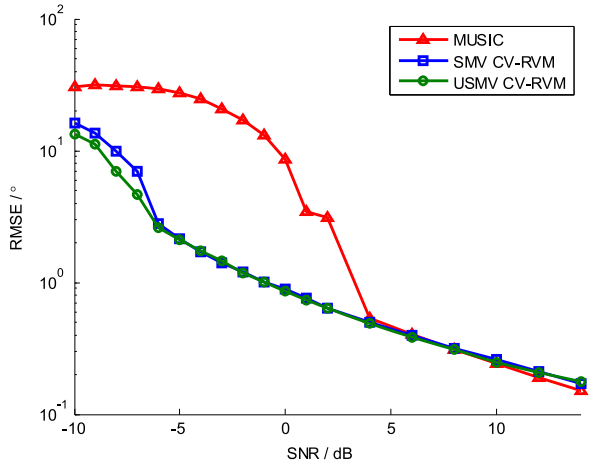


**Fig. 2.** RMSE versus SNR.

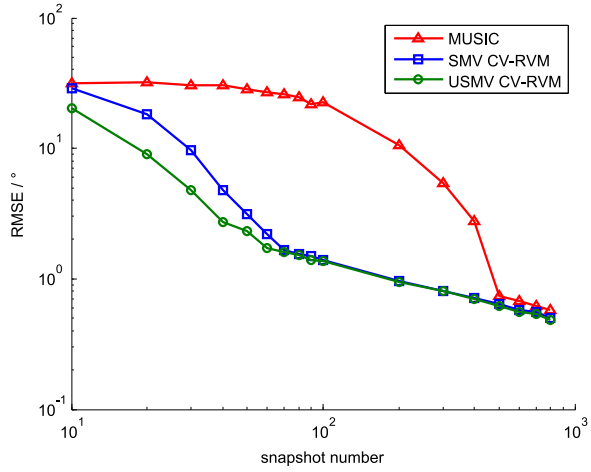


**Fig. 3.** RMSE versus snapshot number.

and USMV CV-RVM versus the SNR and the snapshot number, respectively. The snapshot number is 100 in Fig. 2 and SNR is −3 dB in Fig. 3. It can be concluded from the two figures that USMV CV-RVM has the best performance in low SNR and limited snapshot number scenarios. This is because the unitary transformation doubled the snapshot number. The performance of MUSIC breaks down due to the subspace leakage where some portion of the true signal subspace resides in the estimated noise subspace in low SNR or small snapshot number scenarios [24]. The MUSIC method needs many snapshots or high SNR to obtain an accurate signal subspace.

**Table 1**
Average Computation Time (Seconds).

| Algorithms | SNR | | | | |
|---|---|---|---|---|---|
| | −10 dB | −5 dB | 0 dB | 5 dB | 10 dB |
| MUSIC | 0.0150 | 0.0255 | 0.0456 | 0.0772 | 0.1376 |
| SMVCV-RVM | 2.3882 | 1.9434 | 1.4398 | 1.2453 | 0.9854 |
| USMVCV-RVM | 0.6174 | 0.4633 | 0.3579 | 0.2963 | 0.2318 |

Then we compare the computational cost of MUSIC, SMV CV-RVM, and USMV CV-RVM. We conduct an evaluation of the computational complexity using TIC and TOC instruction in MATLAB. All the simulation results are obtained using the same PC with an Intel i5-3570 processor and 4 GB of RAM, running MATLAB R2013b on 64-bit Windows 7. The average computation time is given in Table 1, which is obtained from 300 Monte Carlo simulations and the snapshot number is 100. It can be seen from Table 1 that the time cost of USMV CV-RVM is largely reduced compared to SMV CV-RVM. This is because the proposed method is implemented in real domain and the unitary transformation further improves the convergence speed.

Then we consider two correlated narrowband signals from directions $-5^\circ + v$ and $5^\circ + v$, and compare the performance of UMMV CV-RVM with SSMUSIC and MMV CV-RVM. The RMSE of the three methods versus SNR and snapshot number are shown in Figs. 4 and 5, respectively. The snapshot number is 50 in Fig. 4 and SNR is −3 dB in Fig. 5. It demonstrates that UMMV CV-RVM has the lowest RMSE, which is due to that the unitary transformation enhances the SNR and it is helpful to de-correlate the correlated signals.

In the last simulation, we show the proposed method can estimate $M-1$ sources. Five uncorrelated signals from directions [−60 −30 0 30 60] impinge on the ULA. The SNR and the snapshot number are 10 dB and 50, respectively. The spatial spectrum of the SMV CV-RVM method is illustrated in Fig. 6, which shows the proposed method can estimate $M-1$ sources.

## 6. Conclusion

To reduce the computational cost of SVM CV-RVM and MMV CV-RVM, the real-valued implementations of SVM CV-RVM and

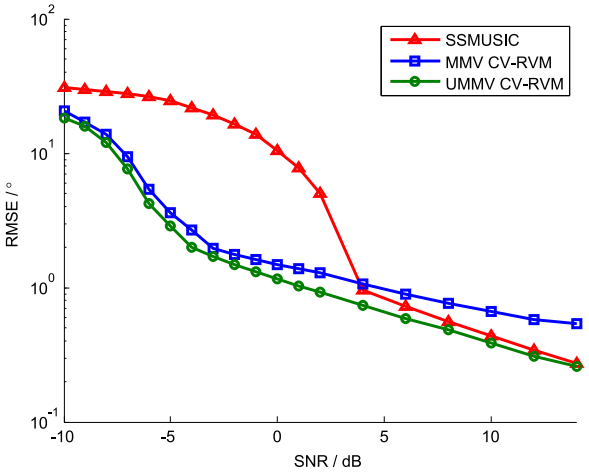


**Fig. 4.** RMSE versus SNR (coherent sources).

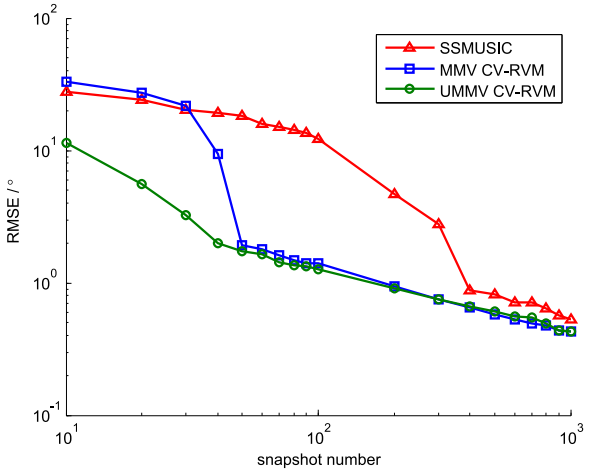


**Fig. 5.** RMSE versus snapshot number (coherent sources).

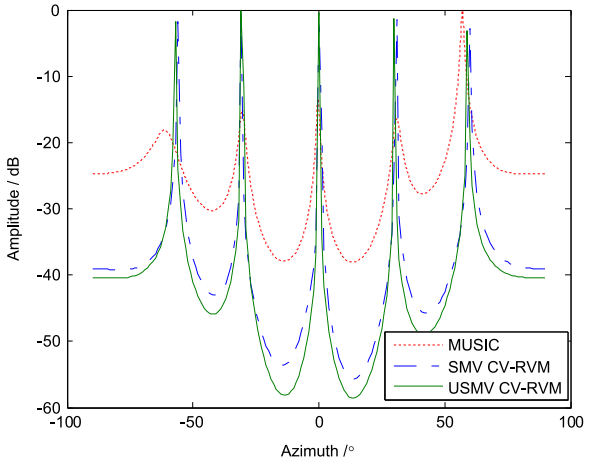


**Fig. 6.** Spatial spectrum of the various methods ($M-1$ sources).

MMV CV-RVM are proposed in this paper, which are named USVM CV-RVM and UMMV CV-RVM, respectively. The covariance matrix of the array output is firstly transformed to a real-valued matrix using unitary transformation. The perturbation of the real-valued matrix is analyzed, and then the real-valued SBL technique for DOA estimation using the real-valued matrix is developed accordingly. USVM – RVM and UMMV CV-RVM can improve the DOA estimation performance compared to the original SVM – RVM and MMV CV-RVM with reduced computational cost. In correlated signals scenarios, the DOA estimation performance of UMMV CV-RVM is shown to be further improved because the unitary transformation is helpful to de-correlate the correlated signals. Simulation results demonstrate the effectiveness of the proposed methods.

## Acknowledgments

This work is supported by National Natural Science Foundation of China(61571344), the Funds of SAST (SAST2015071,SAST2015064).

## Appendix A

The covariance matrix of the perturbation can be represented by

$$\mathrm{E}\left\{\boldsymbol{\xi}_r\boldsymbol{\xi}_r^T\right\}=\frac{1}{4}\left(\boldsymbol{PWP}^H+\boldsymbol{P}^*\boldsymbol{W}^T\boldsymbol{P}^T\right)=\frac{1}{2}\mathrm{Re}\left\{\boldsymbol{PWP}^H\right\}. \tag{43}$$

According to $\boldsymbol{P}=\boldsymbol{T}\otimes\boldsymbol{Q}^H$, we obtain that

$$\begin{aligned}\boldsymbol{PWP}^H&=\frac{1}{N}\left(\boldsymbol{T}\otimes\boldsymbol{Q}^H\right)\left(\boldsymbol{R}^T\otimes\boldsymbol{R}\right)\left(\boldsymbol{T}^H\otimes\boldsymbol{Q}\right)\\&=\frac{1}{N}\left(\boldsymbol{TR}^T\boldsymbol{T}^H\right)\otimes\left(\boldsymbol{Q}^H\boldsymbol{RQ}\right).\end{aligned} \tag{44}$$

Then we can obtain that

$$\begin{aligned}\boldsymbol{TR}^T\boldsymbol{T}^H&=\frac{1}{2}\begin{bmatrix}\boldsymbol{I}&\boldsymbol{J}\\ j\boldsymbol{I}&-j\boldsymbol{J}\end{bmatrix}\begin{bmatrix}\boldsymbol{R}_{11}^T&\boldsymbol{R}_{21}^T\\ \boldsymbol{R}_{12}^T&\boldsymbol{R}_{22}^T\end{bmatrix}\begin{bmatrix}\boldsymbol{I}&\boldsymbol{J}\\ j\boldsymbol{I}&-j\boldsymbol{J}\end{bmatrix}^H\\&=\frac{1}{2}\begin{bmatrix}\boldsymbol{R}_{11}^T+\boldsymbol{JR}_{12}^T+\boldsymbol{R}_{21}^T\boldsymbol{J}+\boldsymbol{JR}_{22}^T\boldsymbol{J}&-j\boldsymbol{R}_{11}^T-j\boldsymbol{JR}_{12}^T+j\boldsymbol{R}_{21}^T\boldsymbol{J}+j\boldsymbol{JR}_{22}^T\boldsymbol{J}\\ j\boldsymbol{R}_{11}^T-j\boldsymbol{JR}_{12}^T+j\boldsymbol{R}_{21}^T\boldsymbol{J}-j\boldsymbol{JR}_{22}^T\boldsymbol{J}&\boldsymbol{R}_{11}^T-\boldsymbol{JR}_{12}^T-\boldsymbol{R}_{21}^T\boldsymbol{J}+\boldsymbol{JR}_{22}^T\boldsymbol{J}\end{bmatrix},\end{aligned} \tag{45}$$

$$\mathrm{diag}\left(\boldsymbol{TR}^T\boldsymbol{T}^H\right)=\left[\mathrm{diag}\left(\boldsymbol{R}_{11}^T+\boldsymbol{JR}_{12}^T+\boldsymbol{R}_{21}^T\boldsymbol{J}+\boldsymbol{JR}_{22}^T\boldsymbol{J}\right)\quad\mathrm{diag}\left(\boldsymbol{R}_{11}^T-\boldsymbol{JR}_{12}^T-\boldsymbol{R}_{21}^T\boldsymbol{J}+\boldsymbol{JR}_{22}^T\boldsymbol{J}\right)\right]. \tag{46}$$

According to the property of the covariance matrix of the sensor output $R=\boldsymbol{R}^H$, we obtain that $\boldsymbol{JR}_{12}^T=\left(\boldsymbol{R}_{21}^T\boldsymbol{J}\right)^H$, and

$$\mathrm{diag}\left(\boldsymbol{JR}_{12}^T\right)=\left(\mathrm{diag}\left(\boldsymbol{R}_{21}^T\boldsymbol{J}\right)\right)^*, \tag{47}$$

$$\mathrm{diag}\left(\boldsymbol{JR}_{22}^T\boldsymbol{J}\right)=\left(\mathrm{diag}\left(\boldsymbol{JR}_{22}^T\boldsymbol{J}\right)\right)^*. \tag{48}$$

Therefore, $\mathrm{diag}\left(\boldsymbol{R}_{11}^T+\boldsymbol{JR}_{12}^T+\boldsymbol{R}_{21}^T\boldsymbol{J}+\boldsymbol{JR}_{22}^T\boldsymbol{J}\right)$ and $\mathrm{diag}\left(\boldsymbol{R}_{11}^T-\boldsymbol{JR}_{12}^T-\boldsymbol{R}_{21}^T\boldsymbol{J}+\boldsymbol{JR}_{22}^T\boldsymbol{J}\right)$ are real-valued vectors, that is $\mathrm{diag}\left(\boldsymbol{TR}^T\boldsymbol{T}^H\right)$ is a real-valued vector.

Thus the $M$ diagonal block of $\boldsymbol{PWP}^H$ are real-valued matrices. The covariance matrix of the perturbation of the $m$th column of the real-valued covariance matrix can be represented by

$$\mathrm{E}\left\{\boldsymbol{\xi}_{rm}\boldsymbol{\xi}_{rm}^T\right\}=\mathrm{Re}\left\{c_{rm}\boldsymbol{Q}^H\boldsymbol{RQ}\right\}=c_{rm}\boldsymbol{R}_r, \tag{49}$$

where $c_{rm}$ is the $m$th diagonal element of the matrix $\frac{1}{2N}\boldsymbol{TR}^T\boldsymbol{T}^H$.

## Appendix B. Supporting information

Supplementary data associated with this article can be found in the online version at http://dx.doi.org/10.1016/j.sigpro.2016.06.002.

## References

[1] H. Krim, M. Viberg, Two decades of array signal processing research: the parametric approach, IEEE Signal Process. Mag. 13 (4) (1996) 67–94.
[2] R.O. Schmidt, Multiple emitter location and signal parameter estimation, IEEE Trans. Antennas Propagat. 34 (3) (1986) 276–280.

[3] R. Roy, T. Kailath, ESPRIT-estimation of signal parameters via rotational invariance techniques, IEEE Trans. Signal Process. 37 (7) (1989) 984–995.
[4] D.L. Donoho, Compressed sensing, IEEE Trans. Inf. Theory 52 (4) (2006) 1289–1306.
[5] M.E. Tipping, Sparse Bayesian learning and the relevance vector machine, J. Mach. Learn. Res. 1 (2001) 211–244.
[6] D. Malioutov, M. Cetin, A.S. Willsky, A sparse signal reconstruction perspective for source localization with sensor arrays, IEEE Trans. Signal Process. 53 (8) (2005) 3010–3022.
[7] M.M. Hyder, K. Mahata, Direction-of-arrival estimation using a mixed L2,0 norm approximation, IEEE Trans. Signal Process. 58 (9) (2010) 4646–4655.
[8] N. Hu, Z. Ye, D. Xu, S. Cao, A sparse recovery algorithm for DOA estimation using weighted subspace fitting, Signal Process. 92 (2012) 2566–2570.
[9] Z. Liu, Z. Huang, Y. Zhou, An efficient maximum likelihood method for direction-of-arrival estimation via sparse bayesian learning, IEEE Trans. Wirel. Comun. 11 (10) (2012) 1–11.
[10] N. Hu, Z. Ye, X. Xu, M. Bao, DOA estimation for sparse array via sparse signal reconstruction, IEEE Trans. Aerosp. Electron. Syst. 49 (2) (2013) 760–773.
[11] J. Zheng, M. Kaveh, Sparse spatial spectral estimation: a covariance fitting algorithm, performance and regularization, IEEE Trans. Signal Process. 61 (11) (2013) 2767–2777.
[12] Z. He, Z. Shi, L. Huang, Covariance sparsity-aware DOA estimation for nonuniform noise, Digit. Signal Process. 28 (2014) 75–81.
[13] Z. Liu, Z. Huang, Y. Zhou, Sparsity-inducing direction finding for narrowband and wideband signals based on array covariance vectors, IEEE Trans. Wirel. Comun. 12 (8) (2013) 3896–3907.
[14] Y. Zhang, Z. Ye, X. Xu, N. Hu, Off-grid DOA estimation using array covariance matrix and block-sparse Bayesian learning, Signal Process. 98 (2014) 197–201.
[15] K.C. Huarng, C.C. Yeh, A unitary transformation method for angle of arrival estimation, IEEE Trans. Acoust., Speech, Signal Process. 39 (4) (1991) 975–977.
[16] M. Haardt, J.A. Nossek, Unitary ESPRIT: how to obtain increasedestimation accuracy with a reduced computational burden, IEEE Trans. Signal Process. 43 (5) (1995) 1232–1242.
[17] A.B. Gershman, P. Stoica, On unitary and forward–backward MODE, Digit. Signal Process. 9 (2) (1999) 67–75.
[18] P. Marius, B.G. Alex, H. Martin, Unitary root-MUSIC with a real-valued eigendecomposition: a theoretical and experimental performance study, IEEE Trans. Signal Process. 48 (5) (2000) 1306–1314.
[19] P. Pal, P.P. Vaidyanathan, Nested arrays: a novel approach to array processing with enhanced degrees of freedom, IEEE Trans. Signal Process. 58 (8) (2010) 4167–4181.
[20] M. Wax, T. Kailath, Detection of signal by information theoretic criteria, IEEE Trans. Acoust., Speech, Signal Process. 33 (2) (1985) 387–392.
[21] Z. Zhang, B. Rao, Sparse signal recovery with temporally correlated source vectors using sparse Bayesian learning, IEEE J. Sel. Top. Signal Process. 99 (2011) 912–926.
[22] J. Chen, X. Huang, Theoretical results on sparse representations of multiple-measurement vectors, IEEE Trans. Signal Process. 54 (12) (2006) 4634–4643.
[23] T.J. Shan, M. Wax, T. Kailath, On spatial smoothing for direction-of-arrival estimation of coherent signals, IEEE Trans. Acoust. Speech Signal Process. 33 (4) (1985) 806–811.
[24] M. Shaghaghi, S.A. Vorobyov, Subspace leakage analysis and improved DOA estimation with small sample size, IEEE Trans. Signal Process. 63 (12) (2015) 3251–3265.